Journal of Catalysis 281 (2011) 177–187

Contents lists available at ScienceDirect

Journal of Catalysis

journal homepage: www.elsevier.com/locate/jcat

Sulfation of metal–organic frameworks: Opportunities for acid catalysis and proton conductivity

Maarten G. Goesten [a], Jana Juan-Alcañiz [a], Enrique V. Ramos-Fernandez [a], K.B. Sai Sankar Gupta [b], Eli Stavitski [c], Herman van Bekkum [a], Jorge Gascon [a,*], Freek Kapteijn [a]

[a] Catalysis Engineering – Chemical Engineering Dept., Delft University of Technology, Julianalaan 136, 2628 BL Delft, The Netherlands
[b] NMR Department, Universiteit Leiden, Einsteinweg 55, Leiden, The Netherlands
[c] National Synchrotron Light Source, Brookhaven National Laboratory, Upton, NY 11973, United States

ARTICLE INFO

Article history:
Received 14 February 2011
Revised 11 April 2011
Accepted 22 April 2011
Available online 24 May 2011

Keywords:
Metal–organic frameworks
MIL-53
MIL-101
Esterification
Proton conductivity
Flexibility

ABSTRACT

A new post-functionalization method for metal–organic frameworks (MOFs) has been developed to introduce acidity for catalysis. Upon treatment with a mixture of triflic anhydride and sulfuric acid, chemically stable MOF structures MIL-101(Cr) and MIL-53(Al) can be sulfated, resulting in a Brønsted sulfoxy acid group attached to up to 50% of the aromatic terephthalate linkers of the structure. The sulfated samples have been extensively characterized by solid-state NMR, XANES, and FTIR spectroscopy. The functionalized acidic frameworks show catalytic activity similar to that of acidic polymers like Nafion® display in the esterification of *n*-butanol with acetic acid ($TOF \sim 1\ min^{-1}$ @ 343 K). Water adsorbs strongly up to 4 molecules per sulfoxy acid group, and an additional 2 molecules are taken up at lower temperatures in the 1-D pore channels of S-MIL-53(Al). The high water content and Brønsted acidity provide the structure S-MIL-53(Al) a high proton conductivity up to moderate temperatures.

1. Introduction

The chemistry of metal–organic frameworks (MOF) has advanced considerably during the last few years. Nowadays, thousands of structures are known [1]. The great topological richness of this new class of materials resulting from the combination of metal ions and organic linkers is without precedent [2].

However, the absence of functionalities other than open metal or weak functional organic sites (e.g., amines) in most of these structures limits to a certain extent their applicability [3,4]. Practical solutions to create functional solids include direct synthesis or post-synthetic functionalization of MOFs [5–7], grafting of active groups on the open metal sites of certain structures [8], and encapsulation of active species [9]. In fact, the incorporation of ligands, including additional functional moieties, is not trivial, since such groups may directly coordinate to the metal ions [10]. One of the current challenges is the development of efficient functionalization methods that can be applied to MOFs without functional organic sites [11] (in many cases, the most stable frameworks), i.e., the direct functionalization of aryl carbons in terephthalate-linked MOFs.

During the last few decades, much effort has been put into the development of super-acidic solid materials such as ion-exchange resins based on sulfonic acid groups [12] or sulfated oxides based on zirconia [13], silica, or alumina [14]. However, the application window of such materials is limited: some exhibit swelling in solvents (polymers) or strong leaching issues (sulfated oxides), while none of them possess a defined porosity. Therefore, the development of nanostructured strongly acidic catalysts is still in the portfolio of materials' researchers.

In principle, MOFs offer a large amount of possibilities for the inclusion of active moieties. Indeed, owing to their hybrid nature, functional groups could be included in such nanostructured materials by applying classical organic chemistry. However, in many cases, the limited chemical stability of MOFs does not allow harsh functionalization conditions, and terephthalate, perhaps the most used ligand in MOF synthesis, is deactivated for electrophilic substitution reactions at its aromatic ring due to the presence of carboxylate groups that diminish the density of electrons in the ring. Traditional sulfonation or sulfation methods [15] are a clear example: MOFs cannot be exposed to high concentrations of sulfuric acid since the framework would be destroyed. In this sense, several groups have tried to include sulfo type of functionalities: Burrows et al. pioneered the incorporation of secondary sulfone moieties by using thiol-tagged linkers followed by a post-synthetic oxidation [16], and Neofotistou et al. used a pre-modified linker already containing secondary sulfones: the ligand 4,4′-bibenzoic

* Corresponding author. Fax: +31 (0) 15 2785006.
E-mail address: j.gascon@tudelft.nl (J. Gascon).

0021-9517/$ - see front matter © 2011 Elsevier Inc. All rights reserved.
doi:10.1016/j.jcat.2011.04.015

acid-2,2′-sulfone [17]. This approach, however, does not introduce acid functionality. Along the same line, Britt et al. reported the post-synthetic modification of an amine containing MOF (IRMOF-3) with sultones, resulting in the opening of the sultone ring and the formation of terminal sulfonic acid groups [18]. In spite of the elegance of this method, sultones are among the most hazardous chemicals, forbidden in most developed countries. Unfortunately, no real applications for sulfonate-containing MOFs have seen the light after this research.

In this work, a different approach has been followed. Here, we report a room-temperature, homogeneously activated method to post-synthetically incorporate sulfoxy moieties into non-functional, chemically, and thermally stable MOFs (i.e., MIL-101(Cr) [19] and MIL-53(Al) [20]). Characterization results demonstrate that by treating these stable MOFs with a mixture of sulfuric acid and trifluoromethanesulfonic anhydride (triflic anhydride), sulfoxy acid moieties are covalently bonded to the aryl carbons of the organic linker. The resulting functionalized MOFs (denoted as S-MIL-101(Cr) and S-MIL-53(Al)) show excellent acid catalytic properties and a high proton conductivity.

2. Experimental

2.1. Preparation of catalysts

All chemicals were obtained from Sigma–Aldrich and were used without further purification. MIL-53(Al) and Nafion® R50 (0.5 mm pellets) were also purchased from Sigma–Aldrich, while MIL-101(Cr) was synthesized following the procedure described elsewhere [19].

Stoichiometric sulfation was carried out with sulfuric acid in the presence of trifluoromethanesulfonic anhydride (triflic anhydride, Tf_2O), using nitromethane (CH_3NO_2) as solvent. The used molar ratio was MOF-incorporated terephthalate/H_2SO_4/Tf_2O = 1:1:1.5. The mixture was continuously stirred in a water bath at room temperature. After 60 min, the solid product was filtered off, rinsed with ultrapure water and acetone, soaked in ethanol for 24 h at 343 K, and stored at 160 °C.

2.2. General characterization techniques

Nitrogen sorption at 77 K was measured in a Quantachrome Autosorb-6B unit gas adsorption analyzer. Specific BET surface area was calculated between 0.05 and 0.15 relative pressures and pore volume at 0.95 relative pressure. Water adsorption isotherms were measured using a Quantachrome Aquadyne DVS gravimetric water sorption analyzer. The crystalline structures were analyzed by X-ray diffraction (XRD) using a Bruker-AXS D5005 with Cu Kα radiation. Thermogravimetric analysis (TGA) of the MOFs was performed by means of a Mettler Toledo TGA/SDTA851e, under flowing air (60 ml/min) at a heating rate of 5 K/min up to 873 K.

The carbon and sulfur mass percentages (elemental analysis) in the MOF were measured in a Leco CS induction oven. The samples were burnt in a continuous stream of O_2, while the formed gases were analyzed by IR. The analysis is performed in duplicate after which the average concentration is reported.

The infrared spectra were obtained using a Thermo Nicolet Nexus FTIR spectrometer. The samples (1 mg) were mixed with KBr and pressed into self-supported pellets (50 mg/cm^2). The spectra were taken in the transmission mode in an *in situ* cell equipped with CaF_2 windows. Prior to the measurements, the samples were degassed in vacuum (10^{-5} mbar) at 473 K for 30 min to remove adsorbed molecules.

Solid-state ^{27}Al, ^{13}C, and ^{1}H NMR studies were performed on a Bruker AV-750 spectrometer with a 17.6 T magnetic field, in which these nuclei resonate at 195.46, 188.64, and 750.13 MHz, respectively. A H/X/Y 2.5 mm MAS probe-head and a standard ZrO_2 rotor spun at 20 kHz were used. For the acquisition of ^{27}Al MAS spectra, the RF field frequency, pulse duration, number of scans, and repetition time were 55 kHz, 1.5 μs, 1024 scans, and 1 s, respectively. The corresponding parameters were 78.1 kHz, 3.2 μs, 32 scans, and 1 s for ^{1}H MAS spectra. For ^{1}H to ^{13}C CPMAS with TPPM decoupling, we used 62.5 and 89 kHz RF field frequencies in the ^{13}C and ^{1}H channels, respectively, for cross-polarization (CP). The contact time was 3 ms, and the repetition time was 2 s for 1024 scans. Chemical shift references (0 ppm) are $Al(NO_3)_3$ in aqueous nitric acid solution for ^{27}Al and TMS for ^{1}H and ^{13}C. ^{27}Al spectra were fitted with the DMFIT software package [21] to obtain approximations for quadrupolar coupling constant C_q and asymmetry factor *eta*.

The sulfur K-edge experiments were carried out at beamline X19b, National Synchrotron Light source (NSLS) at Brookhaven National Laboratory (Upton, New York). Powder samples were finely ground to prevent scattering and mounted on 2.5-μm Mylar film to reduce the self-absorption effect that commonly occurs for thick samples with S content higher than 0.3 wt.%. The incident X-ray energy was scanned over the range from 2430 to 2500 eV with a step size of 0.25 eV. Elemental sulfur (99.998%, Sigma–Aldrich, USA) was used as reference. Sample fluorescence was measured using a PIPS (passivated implanted planar silicon) detector (Canberra Industries, CT).

2.3. Proton conductivity

The proton conductivity of the S-MIL-53(Al) pellets was measured by AC impedance spectroscopy, using an Autolab PGSTAT302N over a range of 10–10^7 Hz with controlled voltage. The pellets, pressed at 5 ton/cm^2, ca. 13.5 mm × 0.9 mm thick, were clamped between two pairs of electrodes and placed in a chamber under controlled humidity and temperature. No recording of bare MIL-53(Al) was made as this material could not be pelletized.

The resistance R of the membrane was derived from the low intersection of the high-frequency semicircle on a complex impedance plane with the real Re(Z) axis. The conductivity is calculated using the relationship $\sigma = d/(R \times S)$, where σ is the conductivity in S cm^{-1}, R the measured resistance of the membrane in Ω, d the distance between the two electrodes in cm, and S the contact surface, in cm^2. The σ values reported are an average of at least three measurements.

2.4. Catalytic tests

The esterification of acetic acid and *n*-butanol was performed without solvent using a mixture with a molar ratio acetic acid/*n*-butanol = 1:1. The mixture was introduced in a round-bottom flask while being stirred under reflux. A ratio of 3 g catalyst per mol of acetic acid was used. After recovering the catalyst, it was filtered, stored at 423 K, and reused.

3. Experimental results

3.1. Characterization

3.1.1. XRD, TGA, and adsorption

After treatment of two spatially different MOF structures, MIL-101(Cr) and MIL-53(Al), using stoichiometric amounts of H_2SO_4 for only 60 min, a C/S weight ratio of 6 was determined by elemental analysis for MIL-53(Al). Assuming mono-sulfation, this would correspond to successful sulfation of a 50% of the aromatic

terephthalate units. In the case of MIL-101(Cr), up to 20% of the linking terephthalate units could be mono-sulfated (one sulfoxy acid moiety per terephthalate linker) under similar reaction conditions. No sulfation was observed of MOFs treated only with Tf_2O or with H_2SO_4 under similar reaction conditions, indicated by Tf_2O-MIL or H_2SO_4-MIL. XRD patterns of the sulfated samples (Fig. 1a) demonstrate that the framework integrity is preserved after this mild post-treatment (despite some minor changes in S-MIL-53 discussed below). TGA results confirm the high thermal stability in air of the resulting materials (Fig. 1b). In Fig. 1c, a comparison of the N_2 adsorption at 77 K between the same samples is depicted. In the case of MIL-101(Cr), nitrogen adsorption reveals a decrease in the specific surface area from ca. 2750 m^2/g to 2230 m^2/g, while the shape of the isotherm remains unchanged after the modification. In the case of MIL-53(Al), the framework is not open for N_2 at 77 K after sulfation and evacuation at 513 K in high vacuum for 12 h. This result points at a large decrease in the pore size of the MIL-53(Al) caused by the volume of the sulfoxy acid groups and their stacking after dehydration, together with the presence of residual water within the framework (about 15 wt.%), as shown in the TGA analyses (Fig. 1b). In order to demonstrate that, after sulfation, the MIL-53(Al) framework retains its intrinsic porosity, adsorption isotherms of H_2O at different temperatures were measured (Fig. 2). Even though the sulfated sample did not show any N_2 uptake at 77 K, water is able to access the pores. Two steps are observed during water adsorption. The onset of the first step clearly depends on the temperature and shifts to lower relative humidities (RH) with increasing temperature, while the adsorbed amount decreased in the case of T = 358 K. The second step occurs close to 100% RH at all instances, indicative of water condensation in the inter-particle space. In every case, a remarkable adsorption–desorption hysteresis occurs. The whole set of isotherms was determined with the same sample, demonstrating the chemical stability of the framework upon (de)hydration. These water isotherms are arguably unique for microporous materials and completely different from the ones reported for non- or differently functionalized MIL-53(Al) [22]. Indeed, the sulfated sample adsorbs twice as much water as unfunctionalized MIL-53(Al) and more than four times the amount adsorbed by amino-functionalized MIL-53(Al) [22].

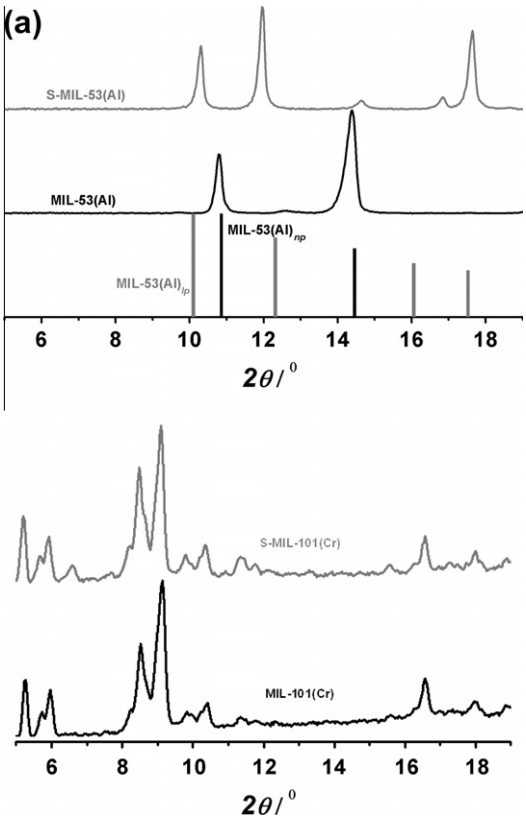

Fig. 1. (a) Powder X-ray diffraction patterns of the sulfated samples compared with that of the bare MOFs. Simulated XRD reflections for the narrow and large pore MIL-53(Al) phases are shown. (b) TGA/DTG analysis of the same samples in air at a heating rate of 5 K/min: samples treated only with Tf_2O or H_2SO_4 are also shown for comparison. (c) N_2 adsorption isotherm at 77 K (closed symbols represent adsorption and open symbols the desorption loop).

3.1.2. Infrared spectroscopy

A complete IR study on the sulfated structures confirms the successful functionalization of both MOFs. Fig. 3 shows a comparison between untreated and sulfated samples. Each material was previously pretreated under vacuum at 573 K for 60 min. Clear differences are already revealed when observing the whole spectra (4000–1000 cm^{-1}). The ν(OH) region (4000–3000 cm^{-1}) exhibits a broad band centered at 3400 cm^{-1} for the sulfated materials, absent in the bare samples. This vibration corresponds to water molecules retained in the pores by strong hydrogen bonds with the sulfoxy acid. Specific sulfoxy acid stretchings can be observed when zooming in at the region between 1800 and 1000 cm^{-1} [23,24].

In the case of MIL-101(Cr), new bands appear at 1170 and 1260 cm^{-1} along with a shoulder at 1430 cm^{-1}, which can be attributed to the O═S═O symmetric and asymmetric stretching modes [23,24]. The peak at 1100 cm^{-1} corresponds to the in-plane skeletal vibration of the benzene rings substituted by a sulfoxy acid group, whereas the 1030 cm^{-1} can be assigned to the S—O stretching vibration [23,25].

In the case of S-MIL-53(Al), double and single S—O bond vibrations of sulfoxy acid groups are observed in the 1350–1000 cm^{-1} region. Upon pretreating the sample, the presence of large amounts of remaining water within the S-MIL-53(Al) framework is evident from the bands appearing in the 3500–2750 cm^{-1} region. The broad band at 3000–2900 cm^{-1} is related to the O—H stretching vibration mode of sulfoxy acid groups associated with cyclic dimers [25]. It is easy to envisage that within the 1-D channel structure of S-MIL-53(Al), sulfoxy acid groups present in opposite channel walls might interact with each other, stacking via hydrogen bonding, as reported for polymers with a high density of sulfonic acid groups [25]. When comparing the IR results with the TGA of S-MIL-53(Al) framework, the water still present in the framework corresponds to the third desorption step, water that is strongly coordinated to the sulfoxy acid moieties.

Fig. 4 shows the comparison between the IR spectra of samples treated with Tf_2O—H_2SO_4 mixtures and samples treated with only one of the reactants (Tf_2O or H_2SO_4), focused on two specific regions of the spectra, namely, 3800–3600 and 1550–950 cm^{-1}. Before recording, the samples were pretreated at 573 K during 60 min in order to remove weakly adsorbed water and differentiate better the spectral features. In the ν(OH) region, two main stretching bands can be observed. MIL-53(Al) (Fig. 4a) reveals only one sharp stretching band at 3700 cm^{-1} related to ν(OH). This result is in line with previous reports, where this peak has been assigned to μ-hydroxo groups [26]. In the case of the modified samples, the stretching band at 3700 cm^{-1} remains, but its intensity decreases dramatically. Some μ-hydroxo groups are free, while other groups interact with guest moieties. Hydrogen bond formation between the μ-hydroxo groups and S═O or —OH moieties (present in sulfoxy groups, H_2SO_4 and Tf_2O) might be the cause of a broad band between 3700 and 3660 cm^{-1} observed in the modified materials. The Tf_2O sample shows a higher intensity at 3660 cm^{-1}, indicating

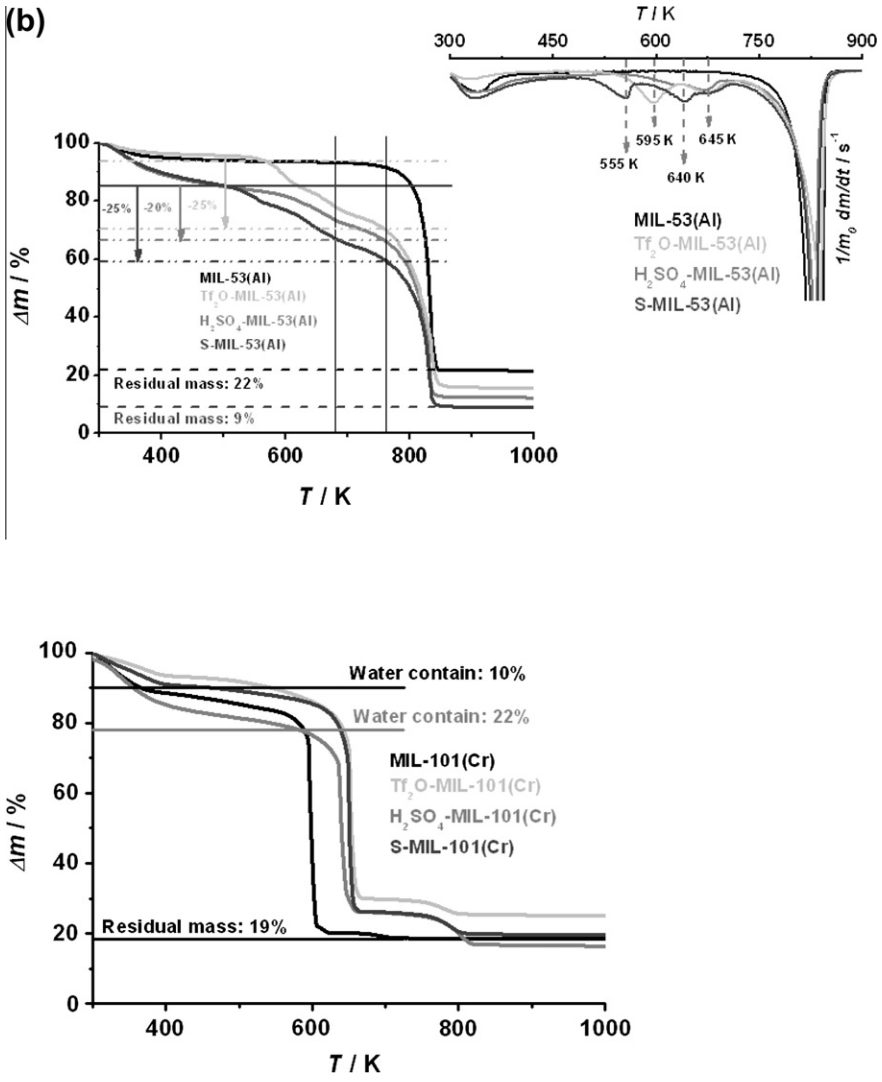

Fig. 1 (*continued*)

a higher density of S═O bonds (4 per molecule, while only 2 per moiety in the sulfated and H_2SO_4 samples).

In the 1550–950 cm^{-1} region, where sulfoxy acid stretchings are present, similar features are observed for the modified materials. The absorption maxima at 1290 and 1165 cm^{-1} are due to the symmetric and asymmetric S═O stretching vibrations, respectively. In contrast, the band at 1110 cm^{-1}, only appearing in the sulfated sample, is related to the benzene rings substituted with an acid sulfoxy group. These results are in agreement with the data obtained for S-MIL-101(Cr).

On the basis of the catalytic activity and the fact that sulfated and their hydrated materials contain hydrated protons [27], IR spectroscopy was applied *in situ* during dehydration of the same samples. At this point, it is of primary importance to show the main differences and similarities between samples sulfated and those treated only with H_2SO_4 or Tf_2O. Fig. 5 shows the IR spectra recorded during the dehydration of the modified and bare materials. The samples were treated at the specified temperature under vacuum for 10 min before spectra were collected. In the case of MIL-53(Al), the solid exhibits a breathing phenomenon upon hydration/dehydration, which involves atomic movements of ~5 Å [20]. In the hydrated form, the pores are slightly deformed due to interactions between the hydrogen atoms of adsorbed water and the μ-hydroxo groups. When water is desorbed, the structure opens [28]. In vacuum at room temperature, three different types of —OH groups (I*, II*, and III*) are present in the sample, apart from the physisorbed water (IV*). The bands at 3660 (II*) and 3610 cm^{-1} (III*) can be assigned to interaction between the μ-hydroxo groups and water moieties in the pores [29]. In addition, the peak at 3700 cm^{-1} shows the ν(OH) of the μ-hydroxo group. In this situation, the pores of the structure are closed. After heating at 373 K under vacuum, the type III* groups have already disappeared with most of the broad water band. As the pretreatment temperature increases, strongly adsorbed water moieties desorb (disappearance of the 3660 cm^{-1} band). When reaching 623 K under vacuum, only the 3700 cm^{-1} band (μ-hydroxo groups) is left.

Fig. 5b shows the spectra obtained during the dehydration of S-MIL-53(Al). At room temperature, two main stretching bands appear: –OH group at 3680 (type V*) and 3660 (type II*) cm^{-1}. In addition, a shoulder is present at 3700 (type I*) related to the free μ-hydroxo group. Upon heating, type I* dominates the spectrum, whereas type II* and V* bands decrease drastically.

Fig. 5c presents the dehydration study of H_2SO_4-MIL-53(Al) sample, showing a similar behavior as S-MIL-53(Al). At room temperature, the main —OH bands observed are V* (at 3680 cm^{-1}) and II* (at 3660 cm^{-1}), with a shoulder at 3700 cm^{-1} (type I*) corresponding to free μ-hydroxo groups. When the pretreatment temperature increases, the absorbance at 3680 cm^{-1} decreases

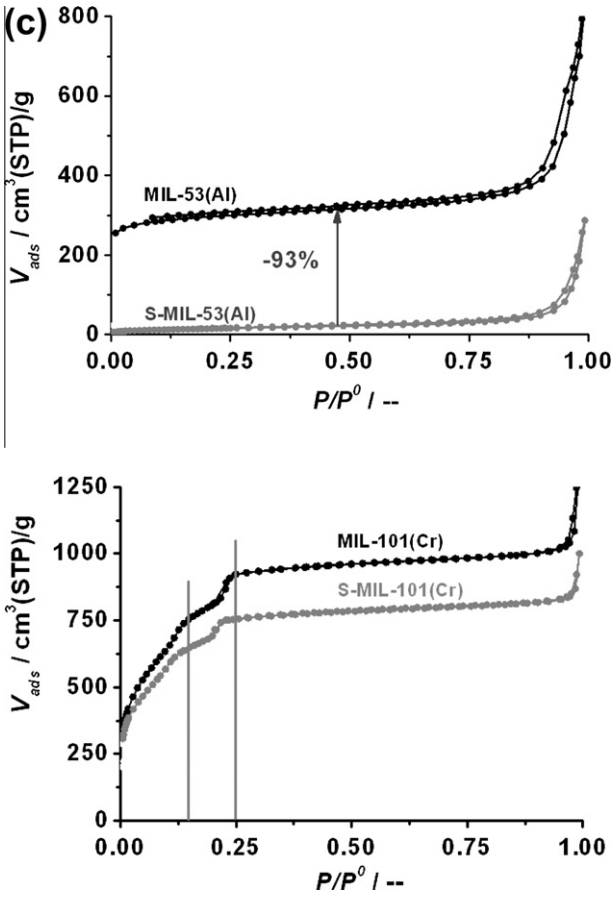

Fig. 1 (*continued*)

significantly, while the band at 3700 cm^{-1} is visible again showing a similar intensity as the also remaining band at 3660 cm^{-1}. Free μ-hydroxo groups are detectable again when most of the water is desorbed by dehydration (third peak in the DTA). Remaining —OH types V* and II* might be associated with —OH groups of H_2SO_4 interacting with water moieties and μ-hydroxo groups.

Fig. 5d shows the dehydration study of Tf_2O-MIL-53(Al). The main stretching band is observed at 3660 cm^{-1} (type II*) with a shoulder at 3680 cm^{-1} (type V*). No free μ-hydroxo groups at 3700 cm^{-1} (type I*) are observed. When the sample is heated, the band at 3680 cm^{-1} is shifted to 3690 cm^{-1}, while the 3660 cm^{-1} (type II*) band decreases in intensity and again the vibration at 3700 cm^{-1} (type I*) appears.

For the bare MIL-53(Al) and Tf_2O-MIL-53(Al) materials, the absorbance at 3610 cm^{-1} disappears upon heating at 373 K under vacuum. In addition, the broad band (centered at 3400 cm^{-1}) associated with υ(OH) of water moieties almost disappears.

In the case of H_2SO_4 and S-MIL-53(Al), the interaction of water with the hydroxyl groups exhibits a different behavior. The peak at 3610 cm^{-1} is not visible due to a broader band centered at 3500 cm^{-1} associated with the υ(OH) of adsorbed water. After pretreating the samples at 473 K under vacuum, the broad band centered at 3500 cm^{-1} is still visible, in contrast to the bare and Tf_2O-MIL-53(Al) samples, showing a much stronger interaction (red shift and desorption at higher temperatures) between water and —OH groups of sulfuric acid and sulfated groups.

3.1.3. Solid-state NMR

In Fig. 6, ^{13}C CPMAS NMR, ^{1}H MAS NMR, and ^{27}Al MAS NMR spectra of S-MIL-53(Al) and unfunctionalized MIL-53(Al) are shown. Similar analyses could not be performed on Cr-based MIL-101 due to the paramagnetic nature of chromium, which sends its unpaired electrons through the linker. Because of this, relaxation is too fast to obtain an acquisition FID.

The ^{13}C CPMAS NMR spectrum shows the removal of free terephthalic acid by the disappearance of the peak at 174 ppm present in the commercial sample. Apparently, the reaction, cleaning, and drying procedure (see experimental) of this sulfation treatment clears out free terephthalic acid. An extra aromatic carbon peak or rather a shoulder at 132–133 ppm is visible. [30] Whether this signal is caused by the aromatic carbon bonded to the sulfate group remains unclear, since Loiseau et al. have reported a similar shoulder for as-synthesized MIL-53(Al) [20]. In their paper, this shoulder

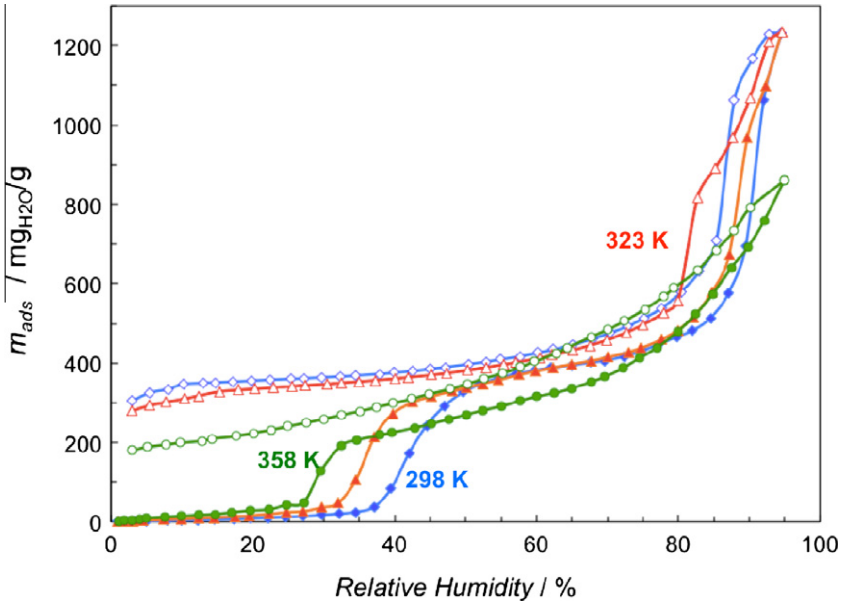

Fig. 2. Water adsorption isotherms of the S-MIL-53(Al) framework at three different temperatures; closed and open symbols correspond to adsorption and desorption, respectively.

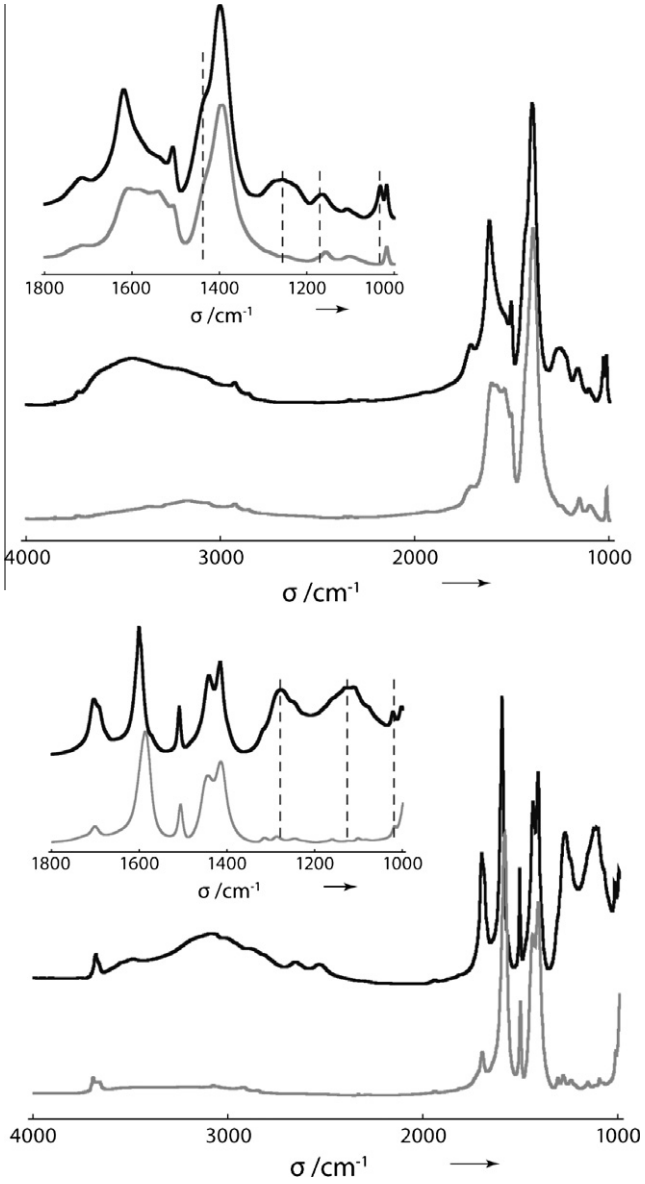

Fig. 3. Comparison between the IR spectra of unfunctionalized (*gray*) and (*black*) S-MIL-101(Cr) (*left*) and S-MIL-53(Al) (*right*).

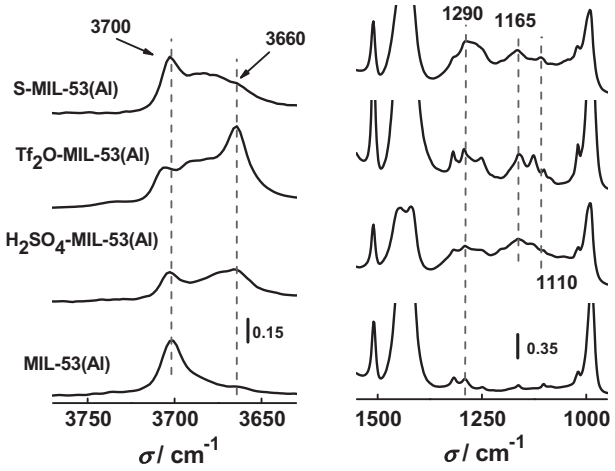

Fig. 4. Infrared spectra in the regions 4000–3000 and 1500–1000 cm^{-1} for MIL-53(Al) sample (sulfated, Tf_2O, and H_2SO_4) treated under vacuum.

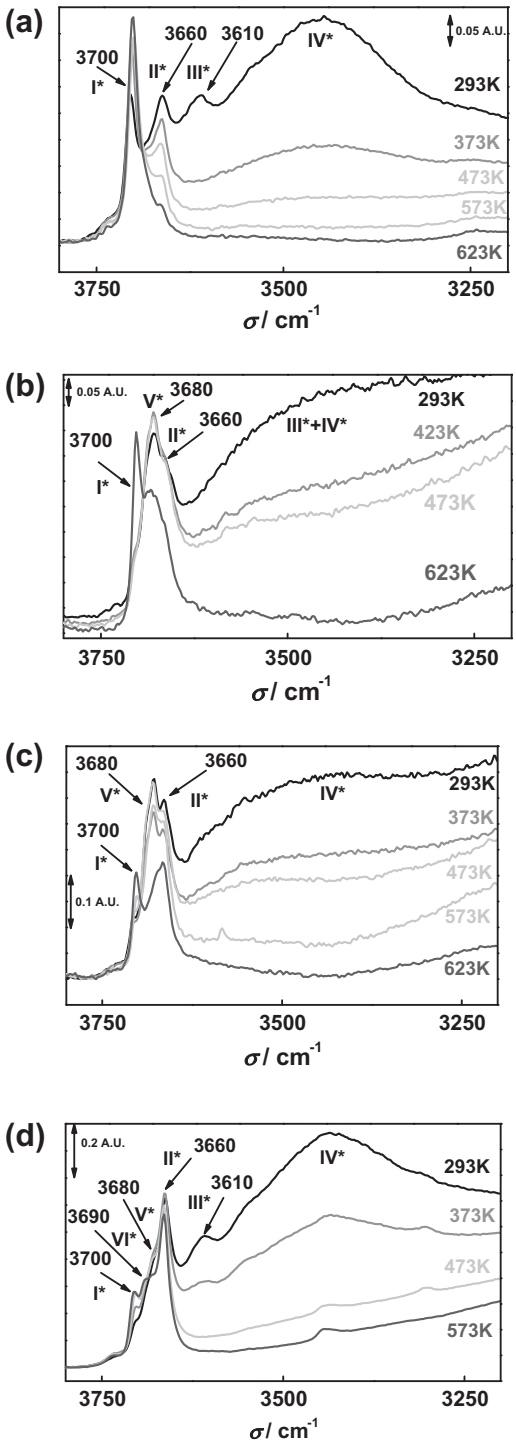

Fig. 5. IR spectra in the ν(OH) (3800–3200 cm^{-1}) region. Study of dehydration by treating under vacuum and heated at different temperatures. (a) Parent MIL-53(Al), (b) S-MIL-53(Al), (c) H_2SO_4-MIL-53(Al) and (d) Tf_2O-MIL-53(Al).

only occurs for as-synthesized MIL-53(Al) as does the terephthalic acid peak at 173–174 ppm, which would suggest it is terephthalic acid giving rise to this signal, but in our case of the S-MIL-53(Al) no free terephthalic acid carbon signal is found. Peaks at 130 and 137 ppm are unfunctionalized aryl carbons bonded to protons.

The ^{1}H MAS NMR spectrum is much more relevant though, with an acidic proton signal at 13–14 ppm. Theoretically, this proton signal could be attributed to free terephthalic acid, but ^{13}C CPMAS experiments and ^{1}H-^{13}C HETCOR experiments (Fig. 7) exclude this.

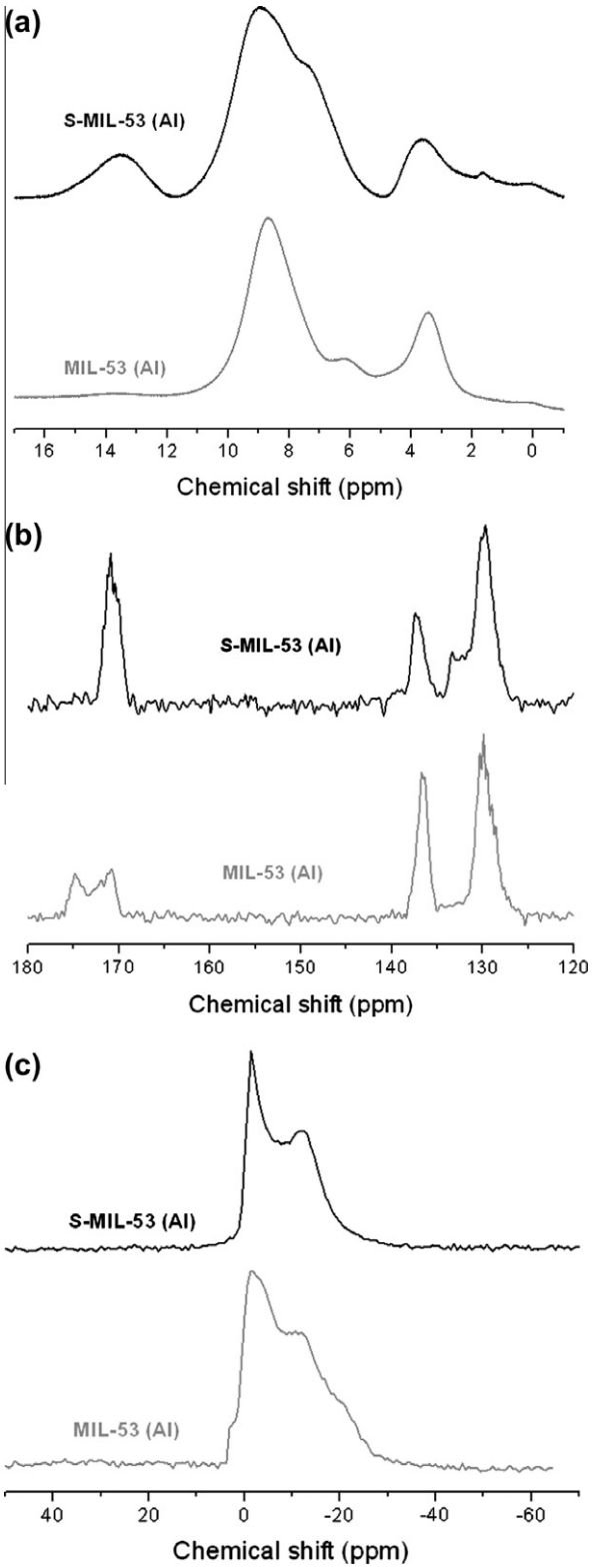

Fig. 6. (a) ^{1}H MAS NMR, (b) ^{13}C CPMAS NMR and (c) ^{27}Al MAS NMR spectra of S-MIL-53(Al) {*black*} and MIL-53(Al) {*gray*}.

In combination with XANES data, later on it is concluded that we deal with a sulfate proton. An extra proton peak at 1.7–1.8 ppm is visible too, which is in perfect correspondence with Al—OH—Al proton signals for heated MIL-53(Al) in Loiseau's work. Apart from that, the peak caused by framework-coordinated water, at 6 ppm for the unfunctionalized sample, is increased and shifted to a higher chemical shift (~8 ppm) for the sulfated sample. This is because the sulfated sample coordinates to more water than the unfunctionalized sample, and sulfate-coordinated water protons are slightly more deshielded, giving rise to a larger chemical shift.

^{27}Al MAS NMR analysis shows interesting results as well as a duplet of peaks is obtained. When fitted with DMFIT, it displays a quadrupolar coupling constant of 12.6 MHz which is significantly larger than the 8.5 and 9.2 MHz coupling constants reported by Lieder et al. [31] in their NMR analysis of MIL-53(Al) with different adsorbents. Quadrupolar coupling constants for solids are correlated with electronic field gradients within the crystal, and it would be reasonable to suppose that sulfoxy acid groups, binding in a non-symmetric way from a crystallographic perspective, enlarge electric field gradients and therefore quadrupolar coupling constants.

Finally, $^{1}H—^{13}C$ HETCOR NMR (Fig. 7) shows that the acidic proton signal is not coming from terephthalic acid, since no cross-peak is visible in that region. The distance between aryl carbons and sulfoxy acid protons was too large to transfer magnetization and obtain cross-correlation. The protons only couple with the aromatic carbons.

3.1.4. X-ray absorption at the sulfur K-edge

So far, we have shown the successful functionalization of the framework with sulfur-containing acidic species. However, the real nature of these sulfur species is not clear yet; indeed, our initial aim was sulfonation (formal oxidation state of sulfur +5) rather than sulfation (formal oxidation of sulfur +6) of the frameworks. In order to unravel the real nature of the active species, sulfur K-edge absorption spectra were recorded in the samples with the higher degree of functionalization (S-MIL-53(Al)). Sulfur K-edge absorption spectra are very sensitive to electronic structure, oxidation state, and the symmetry of the absorbing site. In particular, position of the white line is a very accurate indicator for the oxidation state, spanning across ~11 eV from 2469 eV for cystine (S^{2-}) to 2483 eV for inorganic sulfates (S^{6+}) [32]. The line shape (features in the pre-edge and post-edge regions) may also be used for the identification of the sulfur-containing compounds. The traditional approach for speciation of multicomponent mixtures involves creating a spectral library of the possible components and analyzing the experimental spectra as their linear combination [32,33]. We, however, limit ourselves to determination of the sulfur oxidation state in the sulfated MOF. The XANES region of the K-edge absorption spectra for S-MIL-53(Al) is shown in Fig. 8. Comparison of the white line position (2483 eV) with results reported in the literature [32,33] points out the +6 oxidation state of sulfur (sulfate). This assumption is supported by the experimental spectra of $(NH_4)_2SO_4$ recorded under similar conditions (Fig. 8b) as well as relevant organic compound (chondroitine sulfate [34], Fig. 8c). In all three cases, the absorption maximum appears at nearly the same position. For the organic sulfonate group C—SO_3H, one would expect a shift to lower energy by ~1.5 eV. Indeed, the spectrum of Amberlyst (sulfonic-acid-functionalized polymeric resin) shows a shift of 1.3 eV (Fig. 8d).

3.2. Proton conductivity

Impedance spectroscopy was performed on the S-MIL-53(Al) to characterize its proton conduction properties and to compare them with those of acidic polymers. It turned out that the conductivity of a pellet as a function of temperature in the presence of N_2 saturated with H_2O at room temperature (Fig. 9) lies in the order of magnitude of Nafion® and is several orders of magnitude higher than those reported for other proton-conducting MOFs, albeit measured under dry conditions [35]. Above 353 K, however, the

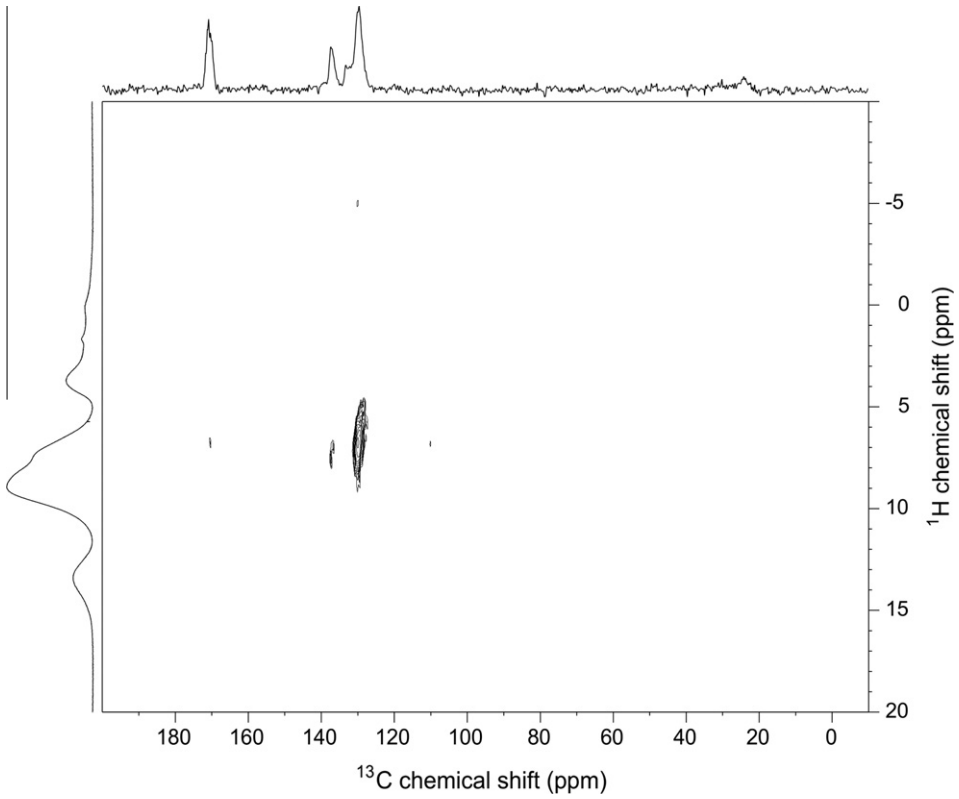

Fig. 7. ^{1}H—^{13}C HETCOR spectra of S-MIL-53 [34].

conductivity drops considerably, suggesting that when water is only adsorbed at the bisulfate groups and not filling up the rest of the framework space, the proton conductivity decreases dramatically. Arguably, in this case, protons can only be conducted through the grain boundaries but not through the dry framework. In any case, the results indicate that model systems like S-MIL-53(Al) represent an excellent playground for studying proton conductivity in confined pores.

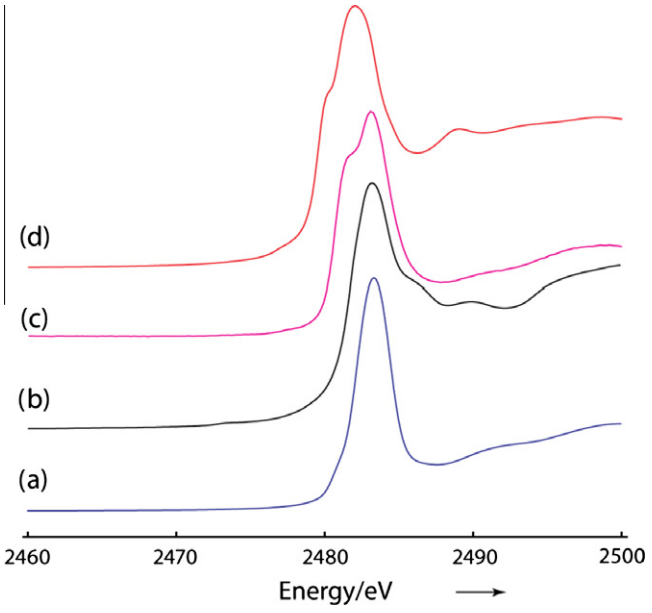

Fig. 8. Sulfur K-edge XANES spectra of (a) Sulfo-MIL-53, (b) $(NH_3)_2SO_4$, (c) chondroitine sulfate and (d) Amberlyst®. Spectra (a), (b) and (d) are recorded in this work, spectrum (c) is adapted from Cuif et al. [30]. All data had been normalized to the height of the white line.

3.3. Esterification of n-butanol and acetic acid

The catalytic activity of the functionalized frameworks has been benchmarked against Nafion® by the liquid-phase stoichiometric esterification of *n*-butanol and acetic acid at low temperatures (343 K). The yield of the only reaction product, butyl acetate, is obtained using the same weight ratio (3 g/mol reactant) of S-MIL-53(Al) and S-MIL-101(Cr) and Nafion® NR50. The functional-

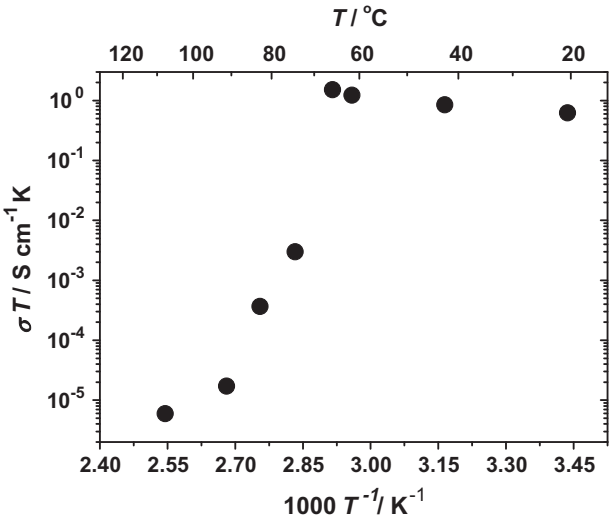

Fig. 9. Conductivity of HSO_4-MIL-53(Al) framework as measured by impedance spectroscopy at different temperatures in the presence of humid N_2 (1.5 wt.% H_2O).

ized samples show a high catalytic activity in the first run, due to adsorbed Tf_2O or H_2SO_4, which are very difficult to eliminate except under reaction conditions. Hence, the performance shown in Fig. 10 is related to the second use of the catalysts in case of the sulfated MOFs and compared with the first use of Nafion® NR50 as standard acid resin. Functionalized S-MIL-53(Al) shows an outstanding performance as acid catalyst and can be recycled without significant loss of activity (Fig. 11). Experiments with unfunctionalized MIL-53(Al) showed the same conversion profile as the blank run, demonstrating that the catalysis can be attributed to the presence of sulfoxy acid groups within the framework. Fig. 12 compares the second use (first reuse) of S-MIL-53(Al) with the same material treated with only one of the reactants (Tf_2O or H_2SO_4). While S-MIL-53(Al) maintains its outstanding performance, Tf_2O and H_2SO_4-MIL-53(Al) drop in activity due to desorption of the active species. These results show the presence of stable active sites in S-MIL-53(Al) formed by the combination of Tf_2O and H_2SO_4 in the sulfation procedure. A slightly higher turnover frequency (*TOF*) per acid group is found for the MOF: 1.0 mol of acetic acid reacts per mol of sulfur per minute against 0.6 for the acidic resin (Table 1). This *TOF* is maintained even after 5 reuses of the S-MIL-53(Al) catalyst.

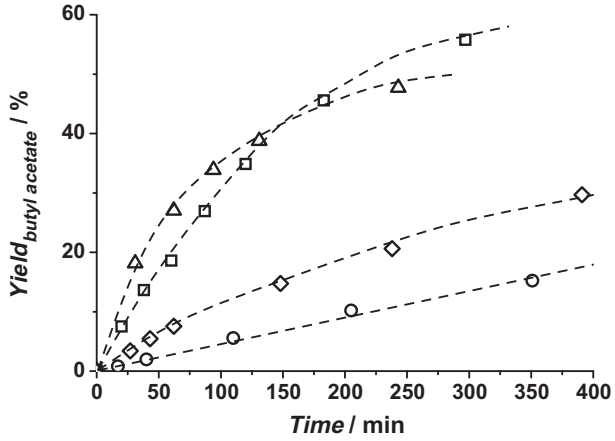

Fig. 10. Esterification of acetic acid with *n*-butanol (molar ratio 1:1) at 343 K with 3 g of catalyst per mol of acetic acid. Yield of butyl acetate as a function of time. (□) Nafion NR50; (Δ) S-MIL-53(Al); (◇) S-MIL-101(Cr) and(○) blank run (no catalyst).

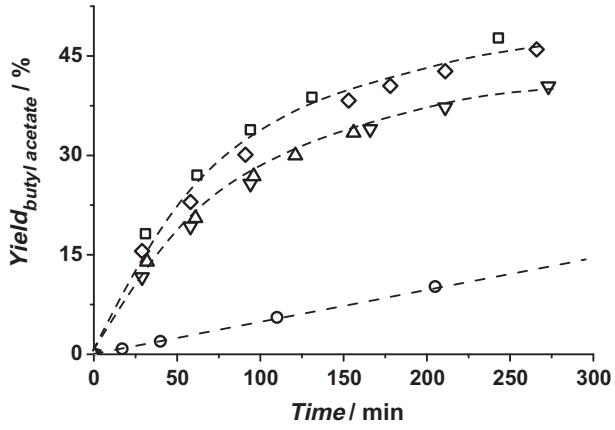

Fig. 11. Esterification of acetic acid with *n*-butanol (molar ratio 1:1) at 343 K with 3 g of catalyst per mol of acetic acid. Yield of butyl acetate as a function of time. (□) First reuse S-MIL-53(Al); (◇) second reuse (▽); third reuse; (Δ) fourth reuse and (○) blank run (no catalyst).

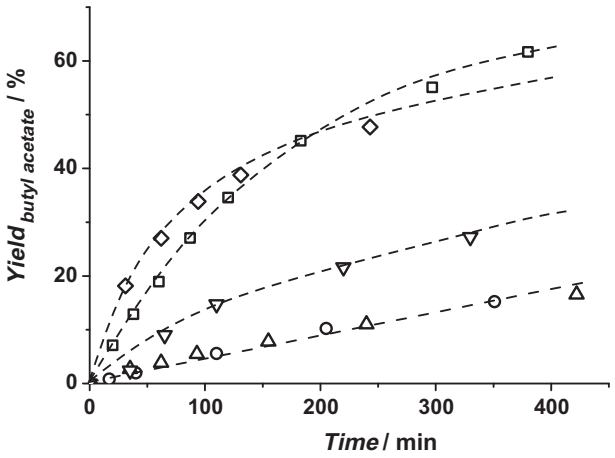

Fig. 12. Esterification of acetic acid with *n*-butanol (molar ratio 1:1) at 343 K with 3 g of catalyst per mol of acetic acid. Yield of butyl acetate as a function of time. (□) Nafion NR50; (◇) first reuse S-MIL-53(Al); (▽) first reuse H_2SO_4-MIL-53(Al); (Δ) first reuse Tf_2O-MIL-53(Al) and (○) blank run (no catalyst).

Table 1
Summary of *TOF* values obtained in esterification of acetic acid with *n*-butanol (molar ratio 1:1) at 343 K with 3 g of catalyst per mol of acetic acid. *TOF*s are based on butyl acetate production after 30 reaction minutes and per mol sulfur for the different samples and reuses.

Catalyst	*TOF* ($mol^{react}\ mol_s^{-1}\ min^{-1}$)
NAFION® NR50	0.63
S-MIL-53(Al) 2nd	1.04
S-MIL-53(Al) 3rd	0.98
S-MIL-53(Al) 4th	0.72
S-MIL-53(Al) 5th	0.85
S-MIL-101(Cr) 2nd	0.55

In the case of S-MIL-101(Cr), a lower *TOF* and activity on a weight basis are obtained, while for samples treated only with Tf_2O or H_2SO_4, no permanent activity was found.

4. Discussion

The extensive characterization of the functionalized samples demonstrates that it is possible to sulfate stable MOF structures using relatively mild conditions. It has to be stressed that the applicability of this method is limited to MOFs with a high chemical stability, similar treatment performed on less stable MOFs like UIO-66 [36] or MIL-68 [37] resulted in the destruction of the MOF.

The presence of sulfoxy acid moieties at the aromatic ring within the functionalized frameworks after post-synthetic treatment is evidenced by NMR and XANES analyses supported by IR evidence from O═S═O and S—O stretching vibrations.

From dehydration and IR experiments, we learnt that the interaction of sulfated samples and samples with adsorbed H_2SO_4 with H_2O and the —OH groups of the structure is, as expected, very similar. However, the new band at 1100 cm^{-1} only appearing in the case of S-MIL-53(Al) together with the NMR results and the fact that for samples treated with only H_2SO_4, the catalytic activity disappears after thorough washing of the material demonstrate that aryl carbon functionalization only takes place when a mixture of Tf_2O and H_2SO_4 is used.

From comparison between the sulfur K-edge absorption spectra of the S-MIL-53(Al) sample and the different standards, it is clear that the oxidation state of sulfur in the MOF sample is +6 rather than +5. The XANES line shape (featuring in the pre-edge and

post-edge regions) is similar to that reported for aryl sulfates (chondroitine sulfate). Together with the absence of any terephthalic acid species in the functionalized material, which is confirmed by $^{1}H—^{13}C$ HETCOR and ^{1}H NMR, this points at sulfoxy acidity. ^{27}Al MAS NMR shows that no aluminum salt residue is present in the sulfated framework and hence no sulfated aluminum oxide clusters. A partial destruction of the framework and possible sulfation of the linker at the carboxylic group is also discarded since it would result in partially coordinated aluminum that should be well visible in the ^{27}Al MAS NMR spectrum.

The mechanistic side of the reaction deserves some special care since we deal with the implementation of a non-ordinary electrophile. The first step is traditional triflic anhydride chemistry in which triflic anhydride reacts with sulfuric acid to produce the mixed anhydride $SO_4H—O—SO_2Tf$. This mixed anhydride then has the sulfur bonded to the Tf group much more strongly polarized than the other sulfur and decomposes into triflate and O^+SO_3H cations, an electrophillic oxygen, and a reagent for electrophilic ring attack and following substitution.

The most common approach for the construction of aryl sulfoxy acids is sulfation of hydroxyl group-containing aromatics using sulfur trioxide–amine complexes or chlorosulfuric acid [38]. Due to the high reactivity of the hydrogen sulfoxy acid proton, sulfated organics are usually produced in the form of alkaline sulfates and it is not common to find sulfate-containing organic compounds. In contrast, when such groups are anchored to porous solids, like inorganic oxides, it has been shown that both SO_4^{2-} and HSO_4^- species are present at the catalyst surface, resulting in a mixed Lewis–Brønsted acid. For example, in the case of sulfated zirconia, the positive charge of exposed Zr^{4+} cations is enhanced by the electron–acceptor nature of adjacent SO_4^{2-} groups and results in strong Lewis acid centers, while hydrogen sulfate/sulfoxy groups and OH^- groups interacting with electron acceptors such as adjacent Zr^{4+} cations have been identified as Brønsted acid sites [14]. In the functionalization of the MOFs, the combination of Tf_2O and sulfuric acid allows the direct formation of sulfoxy acid moieties covalently bonded to the aromatic linkers, while the porosity of the material stabilizes the acidic proton of the sulfoxy acid groups, by interacting and stabilizing its charge in the spatial environment. The sulfoxy acid groups in the MOFs present a good thermal stability. TGA analysis indicates that such functionalities are stable up to 555 K. However, their chemical stability needs attention; a S-MIL-53(Al) sample was boiled in water at pH 10 for 12 h leaving OH groups after hydrolysis.

When it comes to the properties of the sulfated materials, the effect of functionalization on the MIL-53(Al) framework is specifically interesting. MIL-53 is the best-known example of flexible MOFs, which, depending on both the presence of guests and the temperature, evolves from a narrow pore ('closed') to a large pore ('open') form with a variation of the cell volume without any bond breaking [26]. The adsorption of water (Fig. 2) is responsible for the switch between the open and the closed structure, with hydrogen bonding interactions playing the primary role [20]. The difference between this 'breathing' behavior among differently functionalized MIL-53 frameworks and the consequences for separation have recently been reported, demonstrating that the presence of functional organic sites at the aromatic rings strongly disturbs the framework breathing [39,40]. In the case of S-MIL-53(Al), strong hydrogen bonding already occurs in the absence of water. This is in line with the TGA and IR results showing desorption of water at high temperatures and with the XRD pattern depicted in Fig. 1a: after pretreating the sulfated sample at 373 K in inert atmosphere, most of the structure remains in the narrow pore form, as concluded from the half-open/half-closed crystallographic pattern [41]. Only Kusgens et al. [42] reported a somehow similar isotherm shape for the metal–organic framework DUT-4, but in that case, the shape of the isotherm was related to the irreversible collapse of the framework through the addition of water. We attribute the first step in the isotherm to the breathing of the framework: in the low-temperature isotherm, up to six molecules of water are reversibly adsorbed per sulfoxy acid group. The uptake at the highest temperature (358 K) corresponds with around four water molecules per sulfoxy acid moiety. This demonstrates that at lower temperatures, water is adsorbed both at the sulfoxy acid groups and in the remaining pore space, while at increased temperatures, only the sulfoxy acid groups are able to attract water. These adsorption results match the TGA data very well, where similar amounts of released water were observed after sample exposure to ambient conditions. In both cases, the framework has to expand to accommodate the water. In the case of samples treated only with H_2SO_4 or Tf_2O, slightly different TGA profiles are found: none of them show the first H_2O desorption step at around 555 K, related to strongly bonded water to sulfoxy acid moieties.

The proton conduction mechanism in the hydrated S-MIL-53(Al) may be understood as dissociation of the proton from the sulfoxy acid site, transfer of the proton to the aqueous medium, screening by water of the hydrated proton from the conjugate base (sulfoxy anion), and diffusion of the proton in the confined water within the MOF. Regrettably, when the presence of water within the pores of the material decreases, the proton conductivity is lost.

The catalytic results presented in Figs. 10–12 and in Table 1 demonstrate the high activities of the sulfated MOFs, specifically those of the MIL-53(Al) framework, where similar activities as those of Nafion® are found. These results demonstrate that, when anchored to an ordered structure, sulfoxy acid groups are stable and display high acidity. Whether the breathing behavior of S-MIL-53(Al) affects the catalytic performance is not clear. For instance, MIL-53(Fe) breathes through adsorption of different solvents, but the extent of breathing varies upon the nature of the solvent [43]. With regard to the pore opening observed through water adsorption (Fig. 3), it is reasonable to assume that the S-MIL-53(Al) framework will also be open in the reaction mixture, ensuring the full accessibility of sulfoxy acid groups inside the channels.

This work might form the basis for the development of super acid and multifunctional metal–organic frameworks that might find applications in fuel cells, separation of molecules, and catalytic processes.

5. Conclusions

A new post-synthetic functionalization method for metal–organic frameworks has been developed. Upon treatment with a stoichiometric mixture of triflic anhydride and sulfuric acid, it is possible to sulfate the aromatic ring of the terephthalic linker in stable MOF structures. The applicability of this method is, however, limited to MOFs with a high chemical stability like MIL-53(Al) and MIL-101(Cr).

The functionalized frameworks, of which up to 50% of their aromatic ligands were sulfated, show outstanding acid catalytic activity in esterification and thermal stability superior to those of acidic resins. Furthermore, S-MIL-53(Al) shows a high proton conductivity up to moderate temperatures with adsorbed water acting as conductor in a continuous phase.

Acknowledgments

Use of the National Synchrotron Light Source, Brookhaven National Laboratory, was supported by the US Department of Energy, Office of Science, Office of Basic Energy Sciences, under Contract No. DE-AC02-98CH10886. We are thankful to Dr. Syed Khalid for

his help with the XANES measurements. TUDelft is acknowledged for financial support. E.V.R.F. gratefully acknowledges the European Commission for his personal Marie Curie grant. J.G. gratefully acknowledges the Netherlands Science Foundation for his personal VENI grant.

References

[1] G. Ferey, Hybrid porous solids: past, present, future, Chem. Soc. Rev. 37 (2008) 191–214.
[2] J.J. Perry, J.A. Perman, M.J. Zaworotko, Design and synthesis of metal–organic frameworks using metal–organic polyhedra as supermolecular building blocks, Chem. Soc. Rev. 38 (2009) 1400–1417.
[3] D. Farrusseng, S. Aguado, C. Pinel, Metal–organic frameworks: opportunities for catalysis, Angew. Chem., Int. Ed. 48 (2009) 7502–7513.
[4] A. Corma, H. Garcia, F.X.L. Xamena, Engineering metal organic frameworks for heterogeneous catalysis, Chem. Rev. 110 (2010) 4606–4655.
[5] J. Gascon, U. Aktay, M.D. Hernandez-Alonso, G.P.M. van Klink, F. Kapteijn, Amino-based metal–organic frameworks as stable, highly active basic catalysts, J. Catal. 261 (2009) 75–87.
[6] X. Zhang, F.X. LlabrÈs i Xamena, A. Corma, Gold(III)–metal organic framework bridges the gap between homogeneous and heterogeneous gold catalysts, J. Catal. 265 (2009) 155–160.
[7] Z.Q. Wang, S.M. Cohen, Postsynthetic modification of metal–organic frameworks, Chem. Soc. Rev. 38 (2009) 1315–1329.
[8] D.-Y. Hong, Y.K. Hwang, C. Serre, G. Ferey, J.-S. Chang, Porous chromium terephthalate MIL-101 with coordinatively unsaturated sites: surface functionalization, encapsulation, sorption and catalysis, Adv. Funct. Mater. 19 (2009) 1537–1552.
[9] J. Juan-Alcañiz, E.V. Ramos-Fernandez, U. Lafont, J. Gascon, F. Kapteijn, Building MOF bottles around phosphotungstic acid ships: one-pot synthesis of bi-functional polyoxometalate-MIL-101 catalysts, J. Catal. 269 (2010) 229–241.
[10] G.K.H. Shimizu, R. Vaidhyanathan, J.M. Taylor, Phosphonate and sulfonate metal organic frameworks, Chem. Soc. Rev. 38 (2009) 1430–1449.
[11] S.S. Kaye, J.R. Long, Matrix isolation chemistry in a porous metal–organic framework: photochemical substitutions of N_2 and H_2 in $Zn_4O[(\eta 6\text{-}1,4\text{-benzenedicarboxylate})Cr(CO)_3]_3$, J. Am. Chem. Soc. 130 (2007) 806–807.
[12] M.A. Harmer, Q. Sun, Solid acid catalysis using ion-exchange resins, Appl. Catal. A – Gen. 221 (2001) 45–62.
[13] N. Katada, J.-I. Endo, K.-I. Notsu, N. Yasunobu, N. Naito, M. Niwa, Superacidity and catalytic activity of sulfated zirconia, J. Phys. Chem. B 104 (2000) 10321–10328.
[14] M. Marczewski, A. Jakubiak, H. Marczewska, A. Frydrych, M. Gontarz, A. Sniegula, Acidity of sulfated oxides: Al_2O_3, TiO_2 and SiO_2. Application of test reactions, Phys. Chem. Chem. Phys. 6 (2004) 2513–2522.
[15] F. Kucera, J. Jancar, Homogeneous and heterogeneous sulfonation of polymers: a review, Polym. Eng. Sci. 38 (1998) 783–792.
[16] A.D. Burrows, C.G. Frost, M.F. Mahon, C. Richardson, Sulfur-tagged metal–organic frameworks and their post-synthetic oxidation, Chem. Commun. (2009) 4218–4220.
[17] E. Neofotistou, C.D. Malliakas, P.N. Trikalitis, Unprecedented sulfone-functionalized metal–organic frameworks and gas-sorption properties, Chem. – Eur. J. 15 (2009) 4523–4527.
[18] D. Britt, C. Lee, F.J. Uribe-Romo, H. Furukawa, O.M. Yaghi, Ring-opening reactions within porous metal–organic frameworks, Inorg. Chem. 49 (2010) 6387–6389.
[19] G. Ferey, C. Mellot-Draznieks, C. Serre, F. Millange, J. Dutour, S. Surble, I. Margiolaki, A chromium terephthalate-based solid with unusually large pore volumes and surface area, Science 309 (2005) 2040–2042.
[20] T. Loiseau, C. Serre, C. Huguenard, G. Fink, F. Taulelle, M. Henry, T. Bataille, G. Ferey, A rationale for the large breathing of the porous aluminum terephthalate (MIL-53) upon hydration, Chem. – Eur. J. 10 (2004) 1373–1382.
[21] D. Massiot, F. Fayon, M. Capron, I. King, S. Le Calvé, B. Alonso, J.-O. Durand, B. Bujoli, Z. Gan, G. Hoatson, Modelling one- and two-dimensional solid-state NMR spectra, Magn. Reson. Chem. 40 (2002) 70–76.
[22] M. Tagliabue, D. Farrusseng, S. Valencia, S. Aguado, U. Ravon, C. Rizzo, A. Corma, C. Mirodatos, Natural gas treating by selective adsorption: material science and chemical engineering interplay, Chem. Eng. J. 155 (2009) 553–566.
[23] P. Atorngitjawat, R.J. Klein, J. Runt, Dynamics of sulfonated polystyrene copolymers using broadband dielectric spectroscopy, Macromolecules 39 (2006) 1815–1820.
[24] D.S. Warren, A.J. McQuillan, Infrared spectroscopic and DFT vibrational mode study of perfluoro(2-ethoxyethane) sulfonic acid (PES), a model Nafion side-chain molecule, J. Phys. Chem. B 112 (2008) 10535–10543.
[25] B. Ostrowska-Gumkowska, J. Ostrowska-Czubenko, Property–structure relationships in partially sulphonated poly(ethylene terephthalate) – I. Infrared studies, Eur. Polym. J. 30 (1994) 869–874.
[26] C. Serre, F. Millange, C. Thouvenot, M. Nogues, G. Marsolier, D. Louer, G. Ferey, Very large breathing effect in the first nanoporous chromium(III)-based solids: MIL-53 or Cr-III(OH) $\{O_2C\text{–}C_6H_4\text{–}CO_2\}$ $\{HO_2C\text{–}C_6H_4\text{–}CO_2H\}$ H_2O_y, J. Am. Chem. Soc. 124 (2002) 13519–13526.
[27] A. Zecchina, G. Spoto, S. Bordiga, Probing the acid sites in confined spaces of microporous materials by vibrational spectroscopy, Phys. Chem. Chem. Phys. 7 (2005) 1627–1642.
[28] P.L. Llewellyn, S. Bourrelly, C. Serre, Y. Filinchuk, G. Ferey, How hydration drastically improves adsorption selectivity for CO_2 over CH_4 in the flexible chromium terephthalate MIL-53, Angew. Chem., Int. Ed. 45 (2006) 7751–7754.
[29] C. Serre, S. Bourrelly, A. Vimont, N. Ramsahye, G. Maurin, P. Llewellyn, M. Daturi, Y. Filinchuk, O. Leynaud, P. Barnes, G. Férey, An explanation for the very large breathing effect of a metal–organic framework during CO_2 adsorption, Adv. Mater. 19 (2007) 2246–2251.
[30] M.J. Canovas, I. Sobrados, J. Sanz, J.L. Acosta, A. Linares, Proton mobility in hydrated sulfonated polystyrene: NMR and impedance studies, J. Membr. Sci. 280 (2006) 461–469.
[31] C. Lieder, S. Opelt, M. Dyballa, H. Henning, E. Klemm, M. Hunger, Adsorbate effect on $AlO_4(OH)_2$ centers in the metal–organic framework MIL-53 investigated by solid-state NMR spectroscopy, J. Phys. Chem. C 114 (2010) 16596–16602.
[32] G. Sarret, J. Connan, M. Kasrai, G.M. Bancroft, A. Charrié-Duhaut, S. Lemoine, P. Adam, P. Albrecht, L. Eybert-Bérard, Chemical forms of sulfur in geological and archeological asphaltenes from Middle East, France, and Spain determined by sulfur K- and L-edge X-ray absorption near-edge structure spectroscopy, Geochim. Cosmochim. Acta 63 (1999) 3767–3779.
[33] J. Prietzel, J. Thieme, M. Salomé, H. Knicker, Sulfur K-edge XANES spectroscopy reveals differences in sulfur speciation of bulk soils, humic acid, fulvic acid, and particle size separates, Soil Biol. Biochem. 39 (2007) 877–890.
[34] J.-P. Cuif, Y. Dauphin, J. Doucet, M. Salome, J. Susini, XANES mapping of organic sulfate in three scleractinian coral skeletons, Geochim. Cosmochim. Acta 67 (2003) 75–83.
[35] J.A. Hurd, R. Vaidhyanathan, V. Thangadurai, C.I. Ratcliffe, I.L. Moudrakovski, G.K.H. Shimizu, Anhydrous proton conduction at 150 °C in a crystalline metal organic framework, Nat. Chem. 1 (2009) 705–710.
[36] J.H. Cavka, S. Jakobsen, U. Olsbye, N. Guillou, C. Lamberti, S. Bordiga, K.P. Lillerud, A new zirconium inorganic building brick forming metal organic frameworks with exceptional stability, J. Am. Chem. Soc. 130 (2008) 13850–13851.
[37] C. Volkringer, M. Meddouri, T. Loiseau, N. Guillou, J. Marrot, G. Ferey, M. Haouas, F. Taulelle, N. Audebrand, M. Latroche, The Kagome topology of the gallium and indium metal–organic framework types with a MIL-68 structure: synthesis, XRD, solid-state NMR characterizations, and hydrogen adsorption, Inorg. Chem. 47 (2008) 11892–11901.
[38] Y. Liu, I.F.F. Lien, S. Ruttgaizer, P. Dove, S.D. Taylor, Synthesis and protection of aryl sulfates using the 2,2,2-trichloroethyl moiety, Org. Lett. 6 (2003) 209–212.
[39] S. Couck, J.F.M. Denayer, G.V. Baron, T. Remy, J. Gascon, F. Kapteijn, An amine-functionalized MIL-53 metal organic framework with large separation power for CO_2 and CH_4, J. Am. Chem. Soc. 131 (2009) 6326–6327.
[40] S. Couck, J.F.M. Denayer, G.V. Baron, T. Remy, J. Gascon, F. Kapteijn, A pulse chromatographic study of the adsorption properties of the amino-MIL-53 (Al) metal organic framework, Phys. Chem. Chem. Phys. 12 (2010) 9413–9418.
[41] F. Millange, N. Guillou, R.I. Walton, J.M. Greneche, I. Margiolaki, G. Fereya, Effect of the nature of the metal on the breathing steps in MOFs with dynamic frameworks, Chem. Commun. (2008) 4732–4734.
[42] P. Kusgens, M. Rose, I. Senkovska, H. Frode, A. Henschel, S. Siegle, S. Kaskel, Characterization of metal–organic frameworks by water adsorption, Micropor. Mesopor. Mater. 120 (2009) 325–330.
[43] F. Millange, C. Serre, N. Guillou, G. Ferey, R.I. Walton, Structural effects of solvents on the breathing of metal–organic frameworks: an in situ diffraction study, Angew. Chem., Int. Ed. 47 (2008) 4100–4105.